Equations of state and thermodynamic properties of rare-gas solids under pressure calculated using a self-consistent statistical method

A. I. Karasevskii*
Institute for Metal Physics, 36 Vernadsky str., Kiev, 03142, Ukraine

W. B. Holzapfel
Department Physik, Universität Paderborn, D-33095 Paderborn, Germany
(Received 14 January 2003; published 6 June 2003)

Equations of states (EOS's) and thermodynamic properties of rare gas solids (RGS's) under pressure are studied by a statistical method. On the basis of empirical effective two-body interactions for Ar, Kr, and Xe close agreement is obtained with experimental data for the pressure dependencies of the Grüneisen parameter and sound velocities as well as for the temperature dependence of the interatomic distance, the heat capacities, the bulk modulus, and Grüneisen parameter at ambient pressures. All these thermodynamic quantities are finally also calculated for 2, 5, and 10 GPa. Most remarkably a strong suppression of the intrinsic anharmonic contributions to the Gibbs free energy is noticed under strong compression and quantitatively evaluated.

DOI: 10.1103/PhysRevB.67.224301 PACS number(s): 63.70.+h, 64.30.+t, 05.70.Ce, 65.40.−b

I. INTRODUCTION

Thermal contributions to the equations of states (EOS's) for solids under strong compression have received growing attention in recent years for practical reasons related to pressure determination in diamond-anvil high-pressure studies[1–3] as well as in geophysical studies related to the internal geodynamics and density gradients.[2,4] However, the theoretical description of the thermal properties presents still a considerable challenge due to the well-known anharmonicity in the atomic vibrations, which requires especially for large vibrational amplitudes a self-consistent treatment of quasielastic interatomic interactions. Thereby it is well understood[5,6] that the quasiharmonic approximation of the phonon contributions to the thermal pressure cannot describe the experimental data correctly but intrinsic anharmonic contributions have to be taken into account in addition to obtaining an accurate modeling. When these intrinsic anharmonicities are modeled purely on heuristic grounds[7] one is not able to predict the variation of these intrinsic anharmonicities under pressure, which limits the accuracy of these models under stronger compressions. For this reason a statistical model with empirical effective two-body interactions is applied here to study the thermal behavior of rare-gas solids (RGS's) under strong compression in wide ranges of temperature to gain some further insight into the contributions from the intrinsic anharmonicities and into the effects involving self-consistency of the atomic motion in crystals.

In this paper primary attention will be paid at first to the heavier RGS's Ar, Kr, and Xe, where the contributions from quantum motion of the atoms are not so strong as in Ne or He. All the thermophysical data for these RGS's at moderate compression have been reviewed critically in the literature,[8] but more recently, isothermal EOS studies have been extended for solid argon up to 80 GPa,[9–12] for solid krypton up to 55 GPa,[13–16] and for solid xenon up to 75 GPa.[17–20]

While most of the earlier studies on RGS's used only various more or less empirical EOS forms[22,21] in the representation of the experimental data, more recently also first-principles calculations as well as different methods from statistical theories of solids were applied to describe the quasiharmonic atomic motion in crystals.[23–26]

In principle, these statistical methods allow us not only to calculate the EOS's for wide ranges in temperature and pressure, but also to determine all the other thermodynamic properties of these crystals under pressure, however, the usefulness of these models was strongly limited, because quasielastic interatomic interactions and intrinsic anharmonicities of the atomic motions in the crystal were mostly not treated self-consistently in these calculations.

The basis for the theoretical description of the RGS's in the present paper is the statistical method recently proposed for the study of equilibrium properties of solids[27] and successfully applied to the description of thermodynamic properties Ar, Kr, and Xe at ambient pressure.[28] In Sec. II the main results of this statistical theory[27] will be recalled to obtain the basic relations for the EOS of the present RGS. In Sec. III explicit results are compared with the experimental data for Ar, Kr, and Xe. In Sec. IV thermodynamic properties of Ar are presented for pressures of 2, 5, and 10 GPa and compared with ambient pressure data. The pressure dependence of the sound velocities for solid Ar is also compared with experimental results in Sec. IV together with a discussion of the effect of pressure and temperature on the Grüneisen parameter and a comparison with the constraints of the more commonly used Mie-Grüneisen EOS. Results for the changes in the thermal expansion, changes in the isobaric heat capacity, and in the isobaric bulk modulus are also presented in Sec. IV. The effect of pressure on the intrinsic anharmonicity is finally discussed in Sec. V.

II. THE PRESENT STATISTICAL APPROACH

The most difficult task in the statistical approach to the thermodynamic description of crystals is a self-consistent de-

TABLE I. Morse potential parameters and values of the de Boer parameter Λ for RGS's from the literature (Ref. 27).

	α (Å^{-1})	A/k_B (K)	R_0 (Å)	Λ
Ar	1.62	170.76	3.71	0.1360
Kr	1.52	249.08	3.97	0.0767
Xe	1.38	332.04	4.32	0.0457

termination of the phonon frequencies. A self-consistent way to derive an effective quasielastic force constant for the nearest-neighbor interatomic interaction is used in the present approach. The value for this ''effective bond strength'' depends on the distribution of atomic displacements on the nearest lattice sites and, in turn, affects the values of these displacements. To solve this problem, self-consistent phonon (SCP) theories[29–31] have been developed many years ago, whereby iteration processes provide the basis for the determination of a self-consistent interatomic force constant. In order to avoid the difficulties related with the iteration process, a variational approach on the basis of the Gibbs-Bogoliubov functional[32] was introduced[27] to obtain an effective quasielastic bond strength parameter. In this approach a Morse potential between first nearest neighbors is used as an effective interatomic pair interaction in the crystal,

$$u(r_{ij}) = A[e^{-2\alpha(r_{ij}-R_0)} - 2e^{-\alpha(r_{ij}-R_0)}] \tag{1}$$

with the three parameters A, R_0, and α. The values for these parameters are listed in Table I and were determined previously[27] in such a way that the values for the internal energy, the lattice parameter, and the bulk modulus of the RGS at zero temperature and pressure, calculated within the framework of the statistical model,[27] fitted the observed values. In the case of Kr the values of potential parameters were modified with respect to the value of the cohesive energy.[36] The distance between atoms located near the sites R_i and R_j is given here by $r_{ij} = |\mathbf{R}_i - \mathbf{R}_j + \mathbf{q}_i - \mathbf{q}_j|$ and $\mathbf{q}_i$ represents the atomic displacement from the site i.

The quasiharmonic Gibbs-Bogoliubov functional is

$$F_{\mathrm{GB}} = F_0 + \langle U - U_0 \rangle, \tag{2}$$

whereby the

$$\frac{F_0}{NA} = \tau \sum_j \int \ln\left[2\sinh\left(\frac{c\Lambda}{2\tau}\tilde{\omega}_j(\mathbf{K})\right)\right] d\mathbf{K} \tag{3}$$

and

$$\frac{\langle U_0 \rangle}{NA} = \frac{c\Lambda}{4} \sum_j \int \tilde{\omega}_j(\mathbf{K}) \coth\left(\frac{c\Lambda}{2\tau}\tilde{\omega}_j(\mathbf{K})\right) d\mathbf{K} \tag{4}$$

represent the (Helmholtz) free energy and the average internal energy of the quasiharmonic crystal. $\tau = k_B T/A$ is a reduced temperature,

$$\Lambda = \frac{\hbar\alpha}{\sqrt{MA}} \tag{5}$$

is the de Boer parameter for the Morse potential, M and N are the atomic mass and the total number of atoms.

$$c = \left(\frac{\beta_1}{\alpha^2 A}\right)^{1/2} \tag{6}$$

is a dimensionless quasielastic bond parameter and β_1 is an effective force constant for nearest-neighbor atoms.

The average value for the potential energy of the interatomic interaction $\langle U \rangle$ is calculated with the binary distribution function for the atomic displacements[27] and is given by

$$\langle u \rangle = \frac{\langle U \rangle}{AN} = e^{-2b + q(\zeta)/\gamma^*} - 2e^{-b + q(\zeta)/4\gamma^*}, \tag{7}$$

whereby $b = \alpha(R - R_0)$ represents a reduced lattice expansion, R is the nearest-neighbor distance, and

$$q(\zeta) = \frac{2}{1 + \zeta - \frac{7}{2}\zeta^2 + \frac{3}{4}\zeta^3}$$

is a correlation factor, which represents the contribution of the interatomic correlation to the energy of the interatomic interactions, and one may notice that $q(\zeta)$ changes only slowly with temperature from $q_0 \approx 1.87$ at $T = 0$ K to $q \approx 2$ at high temperatures.[27]

$$\zeta = -\frac{c}{\Lambda\gamma^*} \sum_j \int \tilde{\omega}_j(\mathbf{K}) \times \tanh\left[\frac{c\Lambda}{2\tau}\tilde{\omega}_j(\mathbf{K})\right] e_{jx}^2(\mathbf{K}) \cos(2\pi K_x) d\mathbf{K}, \tag{8}$$

is a dimensionless parameter $(0 < \zeta < 1)$, which describes the correlation in the displacement of nearest-neighbor atoms. The inverse value for the width of the atomic localization on a lattice site is characterized by

$$\gamma^* = \frac{c}{\Lambda} \sum_j \int \tilde{\omega}_j(\mathbf{K}) \tanh\left[\frac{c\Lambda}{2\tau}\tilde{\omega}_j(\mathbf{K})\right] e_{jx}^2(\mathbf{K}) d\mathbf{K}, \tag{9}$$

whereby e_{jx} represents the phonon polarization vector for the x direction. The integration in Eqs. (3), (4), (8), and (9) runs over the unit-cell volume of the reciprocal lattice, and $\mathbf{K}$ are reduced components of the wave vector, varying from 0 to 1.[27]

The reduced phonon frequencies of the atomic vibrations $\tilde{\omega}_j(\mathbf{K})$ are determined by the dynamical matrix of the harmonic crystal, i.e., they depend on the lattice structure only. The relation between the scaled frequency $\tilde{\omega}_j(\mathbf{K})$ and the real phonon frequency $\omega_j(\mathbf{K})$ is given by

$$\omega_j(\mathbf{K}) = c\frac{A\Lambda}{\hbar}\tilde{\omega}_j(\mathbf{K}), \tag{10}$$

whereby j represents the specific phonon branch.

The introduction of these reduced variables allows us to parametrize the expression for the free energy (2) with respect to a minimal number of physical parameters describing the thermodynamic properties of the crystal. With these parameters, the quasiharmonic crystal free energy (2) depends

TABLE II. Numerical coefficients used in Eqs. (12)–(17) for the fcc lattice.

n_0	n_1	n_2	n_3	m_0	m_1	p_0	p_1	s_1	s_2	t_1	t_2
2	5/6	0.475	0.296	1/4	−7/96	1/3	1/48	1.928	0.550	1.446	0.092

only on the reduced temperature τ and on the de Boer constant Λ. The internal crystal parameters c and b represent the lattice expansion and the dimensionless effective force constant, determined as equilibrium values minimizing the crystal free energy at the given temperature and pressure.

The contribution from the cubic anharmonicity of the atomic vibrations to the crystal free energy is important especially at high temperature and low pressure. The quasiharmonic expression for the crystal free energy (2) can be corrected in these cases by contributions from cubic anharmonicity of the atomic vibrations in second-order perturbation theory by a term $\Delta F_3(\tau,b)$.[33–35] It has been shown previously,[27,28] that this correction for cubic anharmonicity leads in fact to a good agreement between theory and experiment at zero pressure. The equilibrium state for given values of temperature and pressure corresponds to a minimum of the Gibbs function with respect to b and c. In terms of the present dimensionless functions one has

$$g(\tau,P,c,b)=\varphi_s(\tau,c)+\frac{z}{2}\langle u(\tau,c,b)\rangle+\varphi_3(\tau,c,b)+\tilde{P}w, \tag{11}$$

with $\varphi_s(\tau,c)=(F_0-\langle U_0\rangle)/NA$, $\varphi_3(\tau,c,b)=\Delta F_3/NA$, and $\tilde{P}=P/A\alpha^3$, whereby P is the external pressure and $w=\alpha^3 v$ is the dimensionless atomic volume. In the case of fcc crystals one finds for the atomic volume $v=(R_0+b/\alpha)^3/\sqrt{2}$.

At high ($\tau>c\Lambda$) and low ($\tau<c\Lambda$) temperatures the expression for the Gibbs free energy (11) can be given in explicit forms, which simplify the determination of thermodynamic properties in these temperature ranges.

In the high temperature limit $\tau>c\Lambda$,

$$\gamma^*=\frac{c^2}{\tau}\sum_{l=0}^{3} n_l\left(\frac{c\Lambda}{\tau}\right)^{2l}, \tag{12}$$

$$\zeta=m_0+m_1\left(\frac{c\Lambda}{\tau}\right)^2, \tag{13}$$

$$\varphi_s=\tau\left[p_0+p_1\left(\frac{c\Lambda}{\tau}\right)^4\right]+3\tau\ln\left(\frac{c\Lambda}{\tau}\right), \tag{14}$$

$$\varphi_3=-\frac{a_3}{c^6}\left(e^{-2b+\tau/c^2}-\frac{1}{4}e^{-b+\tau/4c^2}\right)^2\tau^2, \tag{15}$$

whereby $a_3\approx 1.5$. The numerical coefficients n_l, m_l, and p_l, calculated in the case of the fcc lattice, are listed in Table II.

In the case of low temperature $\tau<c\Lambda$,

$$\gamma^*=\frac{c}{\Lambda}\left[s_1-s_2\left(\frac{\tau}{c\Lambda}\right)^4\right], \tag{16}$$

$$\varphi_s=c\Lambda\left[t_1-t_2\left(\frac{\tau}{c\Lambda}\right)^4\right], \tag{17}$$

$$\varphi_3=0,$$

and the correlation parameter for an fcc crystal is $\zeta_0\approx 0.136$ with $q_0\approx 1.87$. The values for the coefficients s_l and t_l for the fcc lattice are also listed in Table II.

In any case, the equilibrium value of effective quasielastic bond strength parameter c and the dimensionless lattice expansion $b=\alpha(R-R_0)$ are determined by the minimization of the Gibbs function (11) with respect to b and c:

$$\left.\frac{\partial g}{\partial b}\right|_{\tau,P,c}=0, \tag{18}$$

$$\left.\frac{\partial g}{\partial c}\right|_{\tau,P,b}=0. \tag{19}$$

III. EQUATION OF STATES

The relations (18) and (19) give the starting point for the determination of the EOS's and for the equilibrium crystals parameters under pressure. A direct relation between the external pressure P and the normalized lattice expansion b, obtained from Eq. (18), is given by the relation (20), in which the parameter q/γ^* and the cubic term φ_3 depend still on τ and c:

$$P=4\sqrt{2}\frac{A\alpha}{(R_0+b/\alpha)^2}\times\left[e^{-2b+q(\zeta)/\gamma^*}-e^{-b+q(\zeta)/4\gamma^*}-\frac{1}{12}\frac{\partial\varphi_3}{\partial b}\right]. \tag{20}$$

Equation (19) gives here a second equation, which determines, in combination with Eq. (18), the equilibrium values of the internal parameters $c_0(\tau,P)$ and $b_0(\tau,P)$.

The variation of the equilibrium value $c_0(\tau,P)$ for Ar under pressure is illustrated in Fig. 1 at two different temperatures ($T=0$ K and $T=295$ K). The steep increase of $c_0(\tau,P)$ at low pressures is typical for RGS's, which show a similarly strong increase in the bulk modulus in this range. The temperature dependence of $c_0(\tau,P)$ at constant P is obviously very small (Fig. 1), however, a temperature dependence of $c_0(v,\tau)$ can be noticed clearly at constant volume, as illustrated in Fig. 2.

One may recall here that $c_0(\tau,P)$ is directly proportional to the (acoustic) Debye temperature,[28] which shows therefore

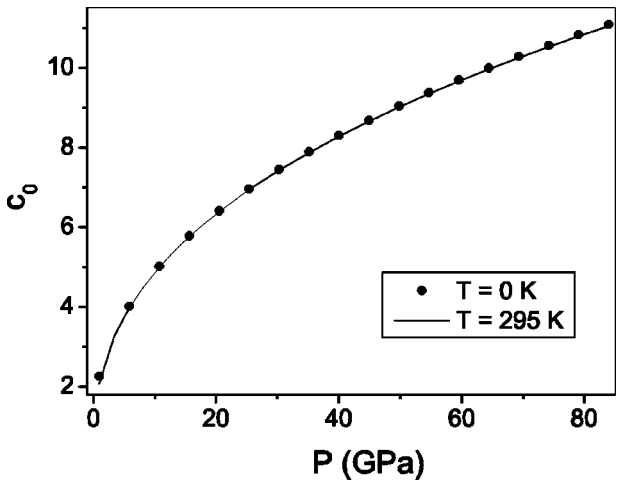

FIG. 1. Effect of pressure on the effective quasielastic bond parameter $c_0(P)$ for Ar at two temperatures, $T=0$ K (circles) and $T=295$ K (solid line).

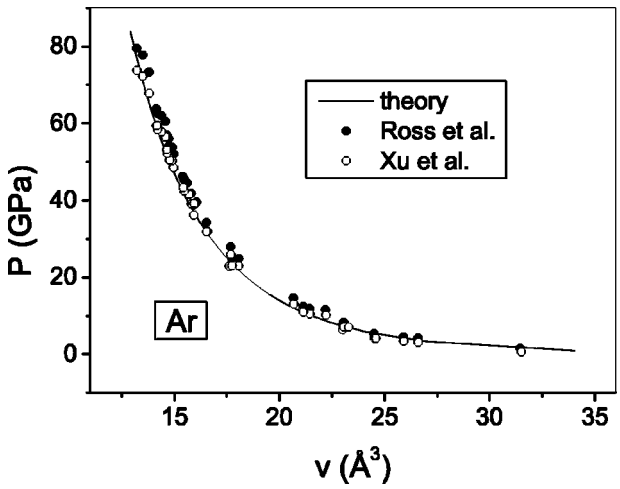

FIG. 3. Calculated EOS for Ar at $T=295$ K (solid line) and experimental data from the literature (Refs. 10 and 11).

the same pressure and temperature dependence as $c_0(\tau,P)$. With the determination of the equilibrium values $c_0(\tau,P)$ and $b_0(\tau,P)$ from the Eqs. (18) and (19) (for given values of P and τ) one can calculate the EOS, which represents the pressure and temperature dependence of the equilibrium volume. For Ar, Kr, and Xe Figs. 3–5 compare the calculated room-temperature isotherms with experimental data.

The good agreement between the experimental and theoretical EOS data in these wide pressure ranges together with the previously published results for the other thermodynamic data of Ar, Kr, and Xe at ambient pressure[27,28] illustrates clearly that the approximation of effective interatomic interactions by the Morse potential (1) with the parameters given in Table I reproduces in the framework of the present statistical model of solids all the available thermodynamic data very reasonably. Therefore this potential can be used for the description of a wide range of microscopic properties for these RGS's in the whole pressure and temperature region covered only partly by the previous experimental studies. However, it should be noted that the parameters in Table I had been deduced from experimental values for the cohesive energy, the bulk modulus, and the interatomic distance at zero pressure and temperature in such a way that the potential represents an effective nearest-neighbor interaction, which may be different from a free atom potential.

One may notice also that the explicit cubic anharmonic contributions to the pressure given by the last term in Eq. (20) are significant only at high temperature and decreases steeply ($\sim c^{-6}$) with increasing pressure.

For the static lattice case, which corresponds to $q/\gamma^*=0$ and $\Lambda=0$, Eq. (20) can be represented in the form of the previously discussed[22,21] effective Morse-type EOS:

$$P(x)=\frac{3K_0}{K_0'-1}\frac{1}{x^2}(e^{-2(K_0'-1)(1-x)}-e^{-(K_0'-1)(1-x)}), \tag{21}$$

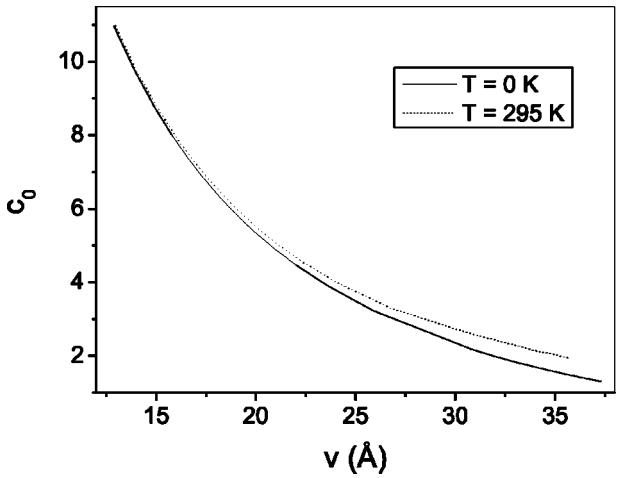

FIG. 2. Effect of volume on the effective quasielastic bond parameter $c_0(v)$ for Ar at two temperatures, $T=0$ K (lower solid line) and $T=295$ K (upper dashed line).

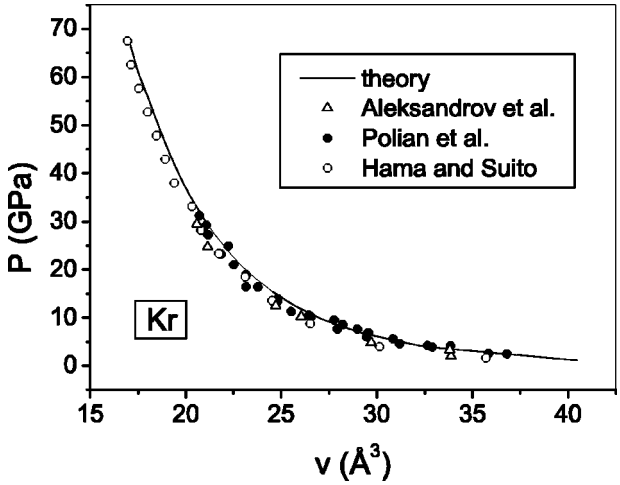

FIG. 4. Calculated EOS for Kr at $T=295$ K (solid line) and data from the literature for experimental (Refs. 13 and 14) and theoretical (Ref. 15) studies.

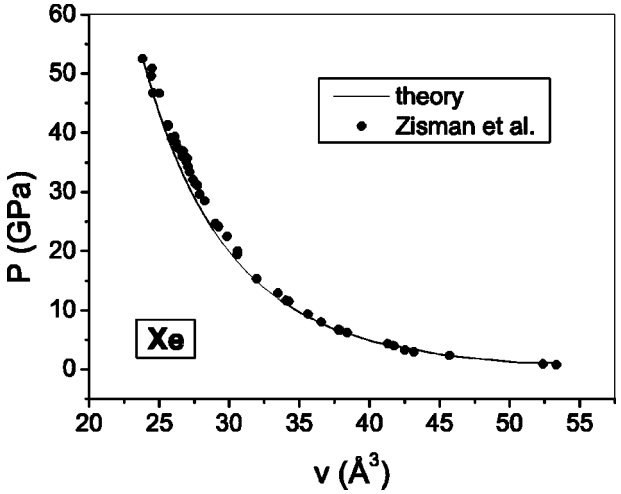

FIG. 5. Calculated EOS for Xe at $T=295$ K (solid line) and experimental data from the literature (Ref. 18).

whereby the parameters of the present approach are easily related to the commonly used values for the bulk modulus at zero pressure, $K_0=(4/3)\sqrt{2}A\alpha^2/R_0$, to its pressure derivative at zero pressure, $K_0'=\alpha R_0+1$, and to the scaled distance parameter, $x=(v/v_0)^{1/3}$, with $v_0=(1/\sqrt{2})R_0^3$ for the zero-pressure volume. From a comparison of Eq. (21) with Eq. (20) one can see that the pressure of the static lattice becomes at high pressure the dominant contribution to the total pressure when

$$|b|\gg q/2\gamma^* \tag{22}$$

and the contributions from both quantum and thermal pressure can then be obtained as leading term $\Delta P(x,\tau)$ in an expansion of Eq. (20) with respect to $q/\gamma^*\ll 1$ in the form

$$\Delta P(x,\tau)=\frac{3K_0}{K_0'-1}\frac{1}{x^2}\left(e^{-2(K_0'-1)(1-x)}-\frac{1}{4}e^{-(K_0'-1)(1-x)}\right)\times\frac{q(\zeta)}{\gamma^*(\tau,c_0)}. \tag{23}$$

The variation of this phonon pressure $\Delta P(x,\tau)$ by compression is illustrated in Fig. 6 by three curves for three different fixed volumes.

First of all one may notice in Fig. 6 that compression of the crystal leads to an increase of the zero-point pressure, which is directly related to the increase of the (acoustic) Debye temperature illustrated by the corresponding increase of $c_0(v,\tau)$ already in Fig. 2. The extension of the flat region at low temperatures reflects in the same way the increase of the Debye temperature. The change in the slopes between the low-pressure and the high-pressure curves represents a special feature, which corresponds to a volume dependence $q_D=(\partial\ln\gamma_{\rm tb}/\partial\ln V)_T<1$ of the corresponding "thermobaric" Grüneisen parameter $\gamma_{\rm tb}$ in contrast to the usual expectation $q_D\geqslant 1$ for the volume dependence of the Grüneisen parameter at moderate pressures.[4] The reason for the distinction between the "thermobaric" Grüneisen parameter[7] used here and the more commonly known Debye-Grüneisen parameter is discussed in the next section.

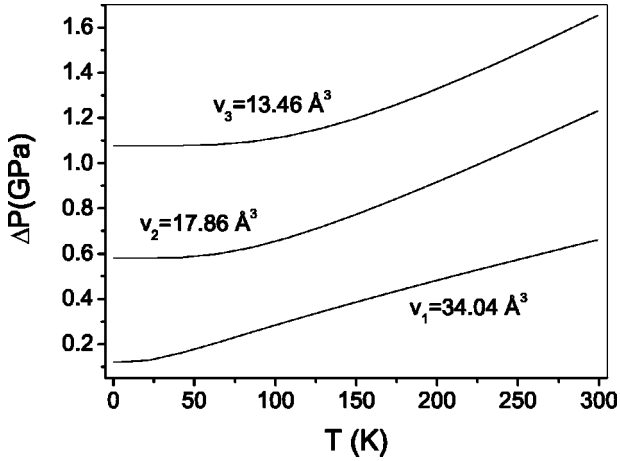

FIG. 6. Isochoric temperature dependence of the phonon pressure at three different volumes.

IV. THERMAL PROPERTIES

As already indicated in the previous section the dominant changes in the thermal properties of the RGS's under pressure are related in the present model to the increase of the quasielastic bond parameter (Figs. 1 and 2), which leads also to increases of the phonon frequencies (10), to an increase of the corresponding Debye temperature, and to a related decrease in the phonon occupation numbers at a given temperature. For nonmetallic crystals like the RGS's the total pressure P can be split into the pressure of the static lattice P_l and an additional phonon contribution, which includes both zero-point and thermal contributions, and one obtains with the internal energy of the phonon subsystem $E_{\rm ph}$

$$P=P_l+(\gamma_{\rm tb}/V)E_{\rm ph}. \tag{24}$$

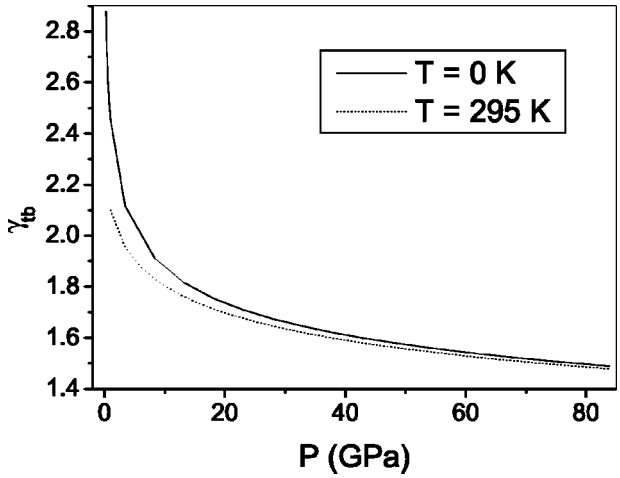

FIG. 7. Effect of pressure on the Grüneisen parameter $\gamma_{\rm tb}$ at two different temperatures: $T=0$ K (upper solid line) and $T=295$ K (lower dashed line).

In the case of a quasiharmonic Debye model, the thermobaric Grüneisen parameter $\gamma_{\rm tb}$, defined by this relation, is identical to the commonly used Debye-Grüneisen parameter $\gamma_D=(\partial \ln \theta_D/\partial \ln V)_T$. However, when θ_D becomes temperature dependent due to effects from (intrinsic) anharmonicity as in the present approach, $\gamma_{\rm tb}$ defined by Eq. (24) becomes

$$\gamma_{\rm tb}=-\frac{(\partial \ln \theta_D/\partial \ln V)_T}{1-(\partial \ln \theta_D/\partial \ln T)_V}. \tag{25}$$

Since the acoustic Debye temperature is directly proportional to $c_0(\tau,b)$,[28]

$$\theta_D=(6\sqrt{2}\pi^2)^{1/3}\langle\kappa_{j\mathbf{k}}\rangle A\Lambda c_0(v,\tau), \tag{26}$$

and Eq. (19) gives an analytical expression for $c_0(\tau,b)$ in the form

$$c_0(\tau,b)=\sqrt{2e^{-2b}-e^{-b}+\sqrt{4e^{-3b}(e^{-b}-1)+e^{-2b}+\frac{\tau}{2}e^{-b}(8e^{-b}-1)}}, \tag{27}$$

one can easily calculate $\gamma_{\rm tb}$ from $c_0(\tau,b)$, and also all the other thermal properties of the crystal under pressure, e.g., thermal expansion and heat capacities. With Eqs. (25)–(27) one obtains for the pressure and volume dependence of $\gamma_{\rm tb}$ the results shown in Figs. 7 and 8, respectively.

Within the quasiharmonic approximation one expects no temperature dependence for $\gamma_{\rm tb}$ at constant volume in contrast to the strong thermal effects seen in Fig. 8, which illustrates that some intrinsic anharmonicity (in addition to the anharmonicity already included in the quasiharmonic approximation) is taken into account by the present approach giving significant contributions in the RGS's especially at low pressures.

For small values of the wave vector $\mathbf{k}$ one can use the relation (10) in the form $\tilde{\omega}_j(\mathbf{k})=\kappa_{j\mathbf{k}}kR$, whereby the coefficients $\kappa_{j\mathbf{k}}$ account also for the different polarizations of the acoustic waves in a given direction, and this relation gives for the pressure and temperature dependence of the sound velocities $u_{j\mathbf{k}}$:

$$u_{j\mathbf{k}}=\kappa_{j\mathbf{k}}\left(\frac{\alpha^2 A}{M}\right)^{1/2}R(T)c_0(P,T). \tag{28}$$

From Eq. (28) sound velocities are calculated for Ar and compared in Fig. 9 with experimental values from the literature.[12]

One can notice, that the values of $\kappa_{j\mathbf{k}}$ along the direction $\langle 111\rangle$ is $2/\sqrt{3}$, giving the highest velocity for the longitudinal acoustic (LA) phonon branch. For the $\langle 100\rangle$ direction $\kappa_{j\mathbf{k}}=1$ gives the lowest velocity for the LA branch in this direction. As one can see from Fig. 9 the agreement between observed[12] and calculated data is rather good for these two LA branches. For the transverse acoustic (TA) branches the differences between experimental data[12] and the present theoretical results are, however, slightly larger. The value $\kappa_{j\mathbf{k}}=1/\sqrt{2}\approx 0.7$ along the $\langle 100\rangle$ direction for largest velocities of the TA branch and $\kappa_{j\mathbf{k}}=0.5$ along the $\langle 110\rangle$ direction for the direction with the lowest velocities of the TA branch do

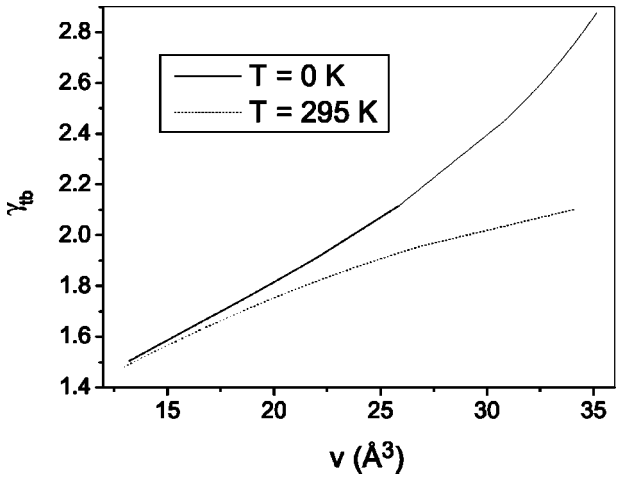

FIG. 8. Effect of volume on the Grüneisen parameter $\gamma_{\rm tb}$ at two different temperature: $T=0$ K (upper solid line) and $T=295$ K (lower dashed line).

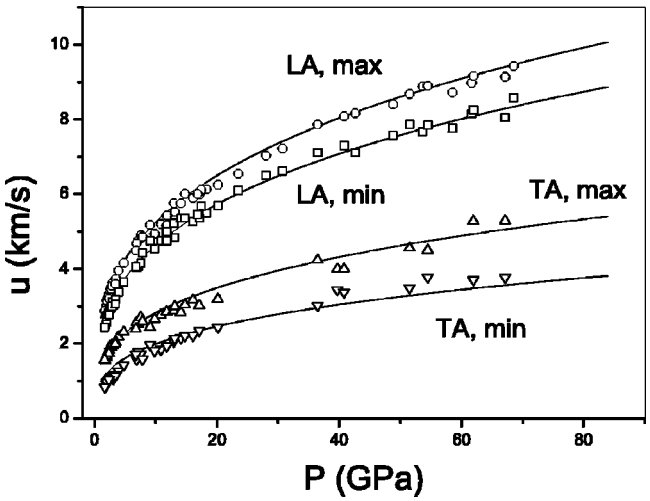

FIG. 9. Effect of pressure on the sound velocities $u_{\rm LA,min}$, $u_{\rm LA,max}$, $u_{\rm TA,max}$, and $u_{\rm TA,min}$ for solid argon. Solid lines are calculated from (28) and symbols represent experimental data from the literature Ref. 12.

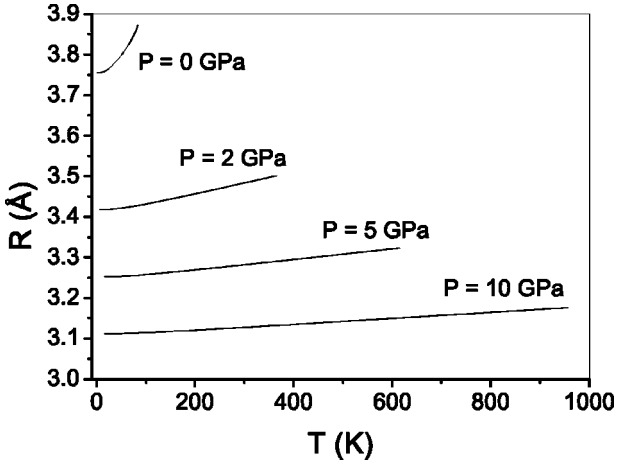

FIG. 10. Temperature dependence of the interatomic distance for Ar at different pressures. The highest temperature for each curve corresponds to the melting point.

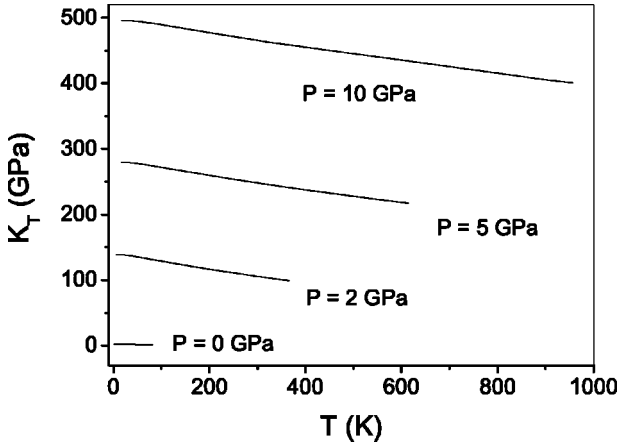

FIG. 12. Temperature dependence of the isothermal bulk modulus for solid Ar at different pressures. The highest temperature for each curve corresponds to the melting point.

not give good agreement with the experimental data,[12] however, a much better agreement between theoretical and experimental data[12] for these TA branches can be obtained with $\kappa_{j\mathbf{k}}=0.61$ and $\kappa_{j\mathbf{k}}=0.43$, respectively. Such a scaling of the calculated velocities for the TA branches can be related to the noncentral character of interatomic interactions.[12]

The average over the sound velocities results in the well-known acoustic, low-temperature limit of the Debye temperature θ_D, given by Eq. (26), and the steep increase in the velocities in Fig. 9 results in a similar increase of θ_D with pressure, which widens the temperature range of the quantum behavior under pressure. Due to the strong decreasing ($\sim c^{-4}$, c^{-6}) of the anharmonic contributions to the free energy of a crystal under pressure the temperature dependence of thermal-expansion coefficient decreases rapidly in the classical high-temperature region ($\tau > c\Lambda$) and the temperature dependence of isothermal bulk modulus K_T becomes linear. These effects are illustrated in Figs. 10–13, showing the temperature dependence for the interatomic distances $R(\tau)$, the isobaric heat capacity C_P, and isothermal bulk modulus K_T, respectively. What is most striking is the strong decrease in the ratio $\kappa=C_P/C_V=K_S/K_T$ under pressure illustrated in Fig. 13.

Effects from intrinsic anharmonicities are also clearly noticed in the temperature dependence for the thermobaric Grüneisen parameter γ_{tb} [defined by Eq. (25)] and in the (different) temperature dependence of the more commonly used ''thermal'' Grüneisen parameter,

$$\gamma_{\mathrm{th}}=\frac{\alpha_V K_T V}{C_V}, \tag{29}$$

where α_V is thermal volume expansion coefficient. Figure 14 illustrates the difference in the temperature dependence of γ_{tb} and γ_{th} at three different pressures.

While the apparent small difference in the two different Grüneisen parameters at low temperatures represents an artifact due to the limited numerical accuracy of the present calculations, the increasing difference at higher temperatures represents the effect of intrinsic anharmonicity taken into

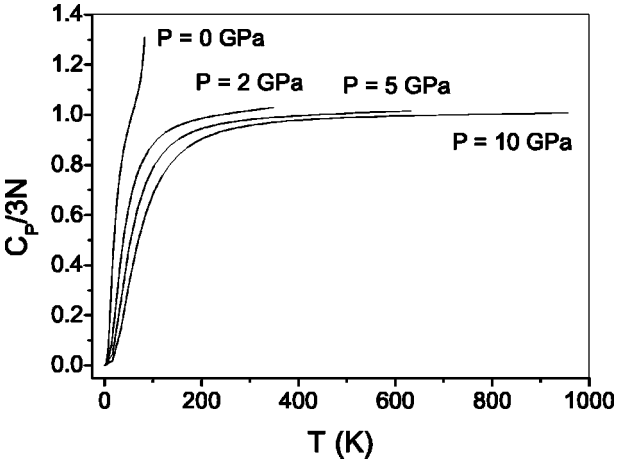

FIG. 11. Temperature dependence of isobaric heat capacity of solid Ar at different pressures. The highest temperature for each curve corresponds to the melting point.

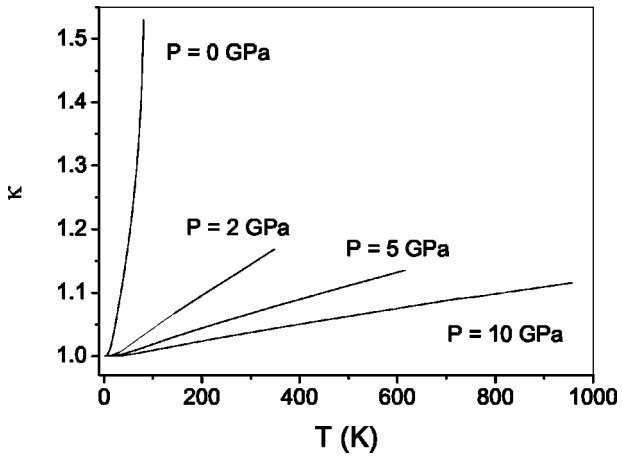

FIG. 13. The temperature dependence of $\kappa=C_P/C_V=K_S/K_T$ at different pressures. The highest temperature for each the curve corresponds to the melting point.

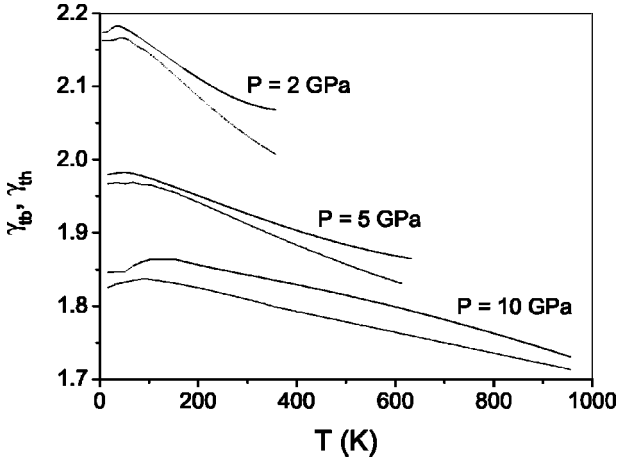

FIG. 14. Temperature dependence of the Grüneisen parameter γ_{tb} (upper solid curve) and γ_{th} (lower dashed curve) at different pressures.

account by the present calculations. One may notice that this difference seems to decrease with increasing pressure.

V. CONCLUSION

The present statistical approach to a calculation of the thermodynamic properties for solids reveals clear differences in the temperature dependences of the different Grüneisen parameters γ_D, γ_{tb}, and γ_{th} due to intrinsic anharmonic contributions, which are very significant in the presently studied RGS's at moderate pressures and elevated temperatures. The strong increase with pressure for the Debye temperature is directly related to the increase in the quasielastic bond parameter $c_0(\tau,P)$ of the present approach (Fig. 1). The temperature $\tau_b = c_0\Lambda$ for the borderline between the quantum and quasiclassical behavior in the thermodynamic properties of solids increases with c_0 and leads to a strong expansion of the quantum regime with pressure, especially in the relatively soft RGS's as illustrated in Figs. 6, 10, and 11 for the phonon pressure, the thermal expansion, and the heat capacity, respectively. The relation (26) with $\langle \kappa_{j\mathbf{k}} \rangle \approx 0.677$ for solids with fcc lattices, like the RGS's, provides a direct link between the quasielastic bond parameter $c_0(\tau,v)$ calculated by the present approach and the commonly used (acoustic) Debye temperature θ_D, which becomes temperature dependent at constant volume in the present approach due to the inclusion of intrinsic anharmonic contributions beyond the quasiharmonic anharmonicities usually represented by a purely volume dependent Debye-Grüneisen parameter γ_D, which becomes temperature dependent at constant volume, when intrinsic anharmonic contributions are taken into account, like in the present approach. Besides the well-known decrease of the quasiharmonic anharmonicity represented by the decrease in pressure (at zero temperature) the present calculation of the temperature dependence for the different Grüneisen parameters, presented in Fig. 14, indicates that the intrinsic anharmonicities decrease also with increasing pressure, at least for the simple RGS's in the pressure range of the present calculations.

In comparison with the recent first-principles calculations for Ar under pressure[26] one may notice that these calculations were restricted to the static lattice case and gave no information on effects from intrinsic anharmonicities and the related thermal effects considered in the present work.

Finally, one may notice that a good description of the thermodynamic properties, including the EOS's of the RGS's, was obtained by the use of an effective nearest-neighbor interaction of the Morse-type with the three parameters of Table I, derived from the interatomic distance, cohesive energy, and the bulk modulus at zero pressure and temperature. Probably such procedure allows an effective potential, in which each atom of the crystal moves, to be determined rather exactly. Since the present statistical method is, however, not limited to the use of an effective Morse-type potential, the present approach can be extended to much higher pressure also by the use of more appropriate effective two-body interactions[22] to the pressure range, where the Morse potential begins to become inadequate.

*Electronic address: akaras@imp.kiev.ua

[1] M. H. Manghnani, L. C. Ming, J. Balog, E. F. Skelton, S. B. Qadri, and D. Schiferl, High Temp.-High Press. **16**, 563 (1984).
[2] W. Utsumi, D. J. Weidner, and R. C. Liebermann, in *Properties of Earth and Planetary Materials at High Pressure and Temperature*, Geophys. Monograph 101 (Am. Geophys. Union, Washington, DC, 1998), p. 327.
[3] W. B. Holzapfel, M. Hartwig, and W. Sievers, J. Phys. Chem. Ref. Data **30**, 515 (2001).
[4] J.-P. Poirier, *Introduction to the Physics of the Earth's Interior* (Cambridge University Press, Cambridge, England, 2000).
[5] P. Choquard, *The Anharmonic Crystal* (Benjamin, New York, 1967).
[6] R. J. Hardy, J. Geophys. Res. **85**, 7011 (1980).
[7] W. B. Holzapfel, J. Phys.: Condens. Matter **14**, 10 525 (2002).
[8] *Rare Gas Solids*, edited by M. L. Klein and J. A. Venables (Academic, New York, 1977).
[9] L. W. Finger, R. M. Hazen, H. K. Mao, P. M. Bell, and G. Zou, Appl. Phys. Lett. **39**, 892 (1981).
[10] J. Xu, H. K. Mao, and P. M. Bell, High Temp.-High Press. **16**, 495 (1984).
[11] M. Ross, H. K. Mao, P. M. Bell, and J. A. Xu, J. Chem. Phys. **85**, 1028 (1986).
[12] H. Shimizu, H. Tashiro, T. Kume, and S. Sasaki, Phys. Rev. Lett. **86**, 4568 (2001).
[13] I. V. Aleksandrov, A. N. Zisman, and S. M. Stishov, Sov. Phys. JETP **65**, 371 (1987).
[14] A. Polian, J. M. Besson, M. Grimsditch, and W. A. Grosshans, Phys. Rev. B **39**, 1332 (1989).
[15] J. Hama and K. Suito, Phys. Lett. A **140**, 117 (1989).
[16] A. Polian, J. P. Itie, E. Dartyge, A. Fontaine, and G. Tourillon, Phys. Rev. B **39**, 3369 (1989).
[17] M. Ross and A. K. McMahan, Phys. Rev. B **21**, 1658 (1980).
[18] A. N. Zisman, I. V. Aleksandrov, and S. M. Stishov, Phys. Rev. B **32**, 484 (1985).
[19] A. P. Jephcoat, H.-k. Mao, L. W. Finger, D. E. Cox, R. J. Henley,

and C.-s. Zha, Phys. Rev. Lett. **59**, 2670 (1987).
[20] W. A. Caldwell, J. H. Nguyen, B. G. Pfrommer, F. Mauri, S. G. Louie, and R. Jeanloz, Science (Washington, DC, U.S.) **77**, 930 (1997).
[21] W. B. Holzapfel, Rep. Prog. Phys. **59**, 29 (1996).
[22] W. B. Holzapfel, High Press. Res. **16**, 81 (1998).
[23] J. H. Kim, T. Ree, and F. H. Ree, J. Chem. Phys. **91**, 3133 (1989).
[24] N. D. Drummond and G. J. Ackland, Phys. Rev. B **65**, 184104 (2002).
[25] E. La Nave, S. Mossa, and F. Sciortino, Phys. Rev. Lett. **88**, 225701 (2002).
[26] T. Iitaka and T. Ebisuzaki, Phys. Rev. B **65**, 012103 (2002).
[27] A. I. Karasevskii and V. V. Lubashenko, Phys. Rev. B **66**, 054302 (2002).
[28] A. I. Karasevskii and W. B. Holzapfel, Low Temp. Phys. (to be published).
[29] N. Boccara, and G. Sarma, Physics (Long Island City, N.Y.) **1**, 219 (1965).
[30] T. R. Koehler, Phys. Rev. Lett. **17**, 89 (1966).
[31] H. Horner, Z. Phys. **205**, 72 (1967).
[32] R. P. Feynman, *Statistical Mechanics* (Benjamian, New York, 1972).
[33] N. S. Gillis, N. R. Werthamer, and T. R. Koehler, Phys. Rev. **165**, 951 (1968).
[34] V. V. Goldman, G. K. Horton, and M. L. Klein, Phys. Rev. Lett. **21**, 1527 (1968).
[35] N. N. Plakida and T. Siklos, Acta Phys. Acad. Sci. Hung. **45**, 37 (1978).
[36] D. A. Young, *Phase Diagrams of the Elements* (University of California Press, Berkeley, 1987).